Microstructural evolution during superplastic deformation of a 7475 Al alloy

DONG H. SHIN*, YEON J. JOO
Department of Metallurgy and Materials Science, Hanyang University, Ansan, Kyunggi-Do, 425-791, South Korea
E-mail:

WOO J. KIM
Department of Metallurgy and Materials Science, Hongik University, Seoul, 121-791, South Korea

CHONG S. LEE
Center for Advanced Materials, Pohang University of Science Technology, Pohang, 790-784, South Korea

Grain refinement of a superplastic 7475 Al alloy is observed at strain rates of $10^{-2}\,s^{-1}$ or higher. Metallographic observation shows that the average grain size is changed from 14 μm to 10 μm after 100% elongation. Two-stage strain-rate tests were performed on the 7475 Al alloy to correlate grain refinement with an improvement of superplasticity. The optimum first strain rate and strain in the first stage were determined through tensile superplastic tests. Superplasticity was improved significantly through two-stage strain-rate testing. This is believed to be related to the refinement of the initial grains at high strain rate. The specimen tested at a strain rate of $2.1 \times 10^{-4}\,s^{-1}$ revealed dispersoid-free zones (DFZs) near grain boundaries normal to the stress axis. When a higher strain rate was applied to the specimens with DFZs, no grain refinement was observed. The absence of grain refinement is due to the concentration of plastic deformation in the weak DFZs. © *1998 Kluwer Academic Publishers*

1. Introduction

Following appropriate thermomechanical processing (TMP), the fine grain microstructure in aluminium alloys required for superplasticity may be obtained through static or dynamic recrystallization. Static recrystallization produces a fine grain structure prior to superplastic deformation, whereas dynamic recrystallization forms a fine grain structure during the early stages of superplastic deformation. The 7000 series aluminium alloys are subject to the former procedures [1, 2], known as the "Rockwell process", whereas the Suprals [3] and 8090 Al–Li alloy [4] undergo dynamic recrystallization.

Superplasticity in aluminium alloys can be improved by two techniques. The first one is a modification of the thermomechanical processing before testing. For example, our previous work [2] has indicated that superplasticity in 7475 Al alloy could be enhanced by a new double recrystallization process. The second is a change in the testing method after TMP. For example, this method includes a two-stage strain-rate test [5] and long-term holding at the superplastic temperature [6]. In the two-stage strain-rate test, the tensile sample was tested by changing from a higher strain rate to lower one. The superplasticity of a 8091 Al–Li alloy was enhanced by this method [5].

In the previous paper [2] on superplastic 7475 Al alloy, there was a particular feature, that is, the presence of dispersoid-free zones (DFZs) adjacent to certain grain boundaries. After the superplastic tests, several specimens revealed large zones free of dispersoid particles, occasionally, as large at 5 μm across. This fact suggests that the occurrence of DFZs may be related to the superplastic deformation mechanism [2].

The purposes of this work were: (1) to correlate grain refinement with an improvement in superplasticity for a 7475 Al alloy using the two-stage strain-rate test, and (2) to investigate the microstructural aspects of the superplastic 7475 Al alloy.

2. Experimental procedure

The 7475 Al alloy was supplied in the form of 10 mm plate. The composition (wt %) is 0.05 Si, 0.06 Fe, 1.43 Cu, 2.4 Mg, 0.2 Cr, and 5.96 Zn.

* Jointly affiliated with the Center for Advanced Aerospace Materials, Pohang University of Science and Technology, Pohang, 790-784, South Korea.

The thermomechanical process used in this study is similar to that developed for 7000 series aluminium alloys [1]. The steps involved in the procedure were: (1) solution treatment at 480 °C for 5 h followed by water quenching; (2) overageing at 400 °C for 8 h; (3) warm rolling at 200 °C; and (4) discontinuous recrystallization at 480 °C for 0.5 h. After this treatment, the average grain size was approximately 14 μm.

Tensile specimens of 8 mm gauge length were tested at 516 °C in an argon (purity, 99.9%) atmosphere using an Instron testing machine. Initial engineering strain rates ranging from 6.3×10^{-5} to $2.1 \times 10^{-2}\ s^{-1}$ were used, and the elongation-to-failure was recorded for each test.

To establish the mechanical behaviour at both low and high stresses, the strain-rate change technique, as well as uninterrupted tests, was adopted. In the strain-rate change tests, the initial rates of crosshead displacement were abruptly changed in one or two steps to those predetermined, either when the maximum load was recorded after the rate was increased, or when a plateau region was obtained after the rate was decreased [7].

3. Results and discussion

The stress–strain rate data for the 7475 Al alloy at a superplastic temperature of 516 °C are presented in Fig. 1. The strain-rate sensitivity, m, that is, the reciprocal of the slope in Fig. 1, is $m = 0.5$ at low and intermediate strain rates. Sherby and Wadsworth [8] used phenomenological relations and concluded that the GBS accommodated by slip ($m = 0.5$) is the most probable mechanism for deformation during superplastic flow of fine-grained materials, which agrees with our result. In the previous work of Shin *et al.* [9], it was shown that Hayden's model [10], one of the GBS models based on GBS accommodated by slip, was close to the experimental data of the superplastic 7475 Al alloy. At $\dot{\varepsilon} > 10^{-2}\ s^{-1}$, the slope in Fig. 1 changes to a lower value of 0.2 (stress exponent $n = 5$), and this implies dislocation slip controls plastic flow [8, 11].

Fig. 2 shows the result of elongation-to-failure tests for the present alloy as a function of strain rate at 516 °C. The results of Fig. 2 show that as the strain rate decreases, the elongation increases. The superplastic 7475 Al alloy shows the elongation-to-failure to be 360% and 720% at an initial strain rate of 1.3×10^{-3} and $2.1 \times 10^{-4}\ s^{-1}$, respectively. The decrease in tensile ductility at high strain rates can be attributed to a decrease in m value and an increase of cavitation activity that prevails as flow stress (strain rate) is increased.

3.1. Deformation at high strain rate

Fig. 3a–d are optical micrographs of the same region in a specimen deformed at a high strain rate of $2.1 \times 10^{-2}\ s^{-1}$ to elongations of 5%, 20%, 45% and 60%, respectively. These micrographs show two unique microstructural features. The first is the formation of slip bands within grains. This is evidence of high dislocation activity in the interior of the grains during deformation, indicating that slip occurred extensively during deformation. The second is the breaking up of coarse grains with deformation (for example, see A and B). This topological change is frequently detected on coarse grains (30–50 μm diameter). As a result, the grains are changed to the equiaxed shape.

Fig. 4a–c show scanning electron micrographs of the same region in a specimen deformed at a strain rate of $2.1 \times 10^{-2}\ s^{-1}$ to elongations of 5%, 45% and 100%, respectively. These micrographs also show that refining of the coarse grains occurs at high strain rate for the statically recrystallized superplastic 7475 Al alloy (for example, see A). The average grain-size distribution is changed from 14 μm to 10 μm.

When the crystalline materials are deformed at elevated temperatures, the accumulated dislocations are continuously destroyed by two separate processes. The two processes are dynamic recovery and dynamic

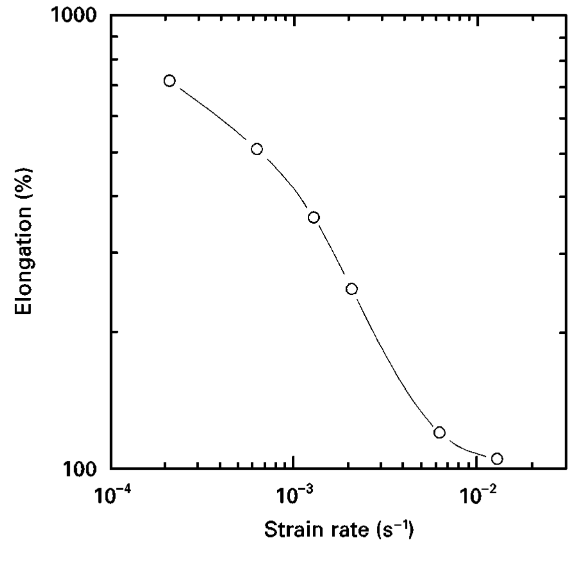

Figure 1 Strain rate as a function of stress for 7475 Al alloy at 516 °C, 14 μm grain diameter.

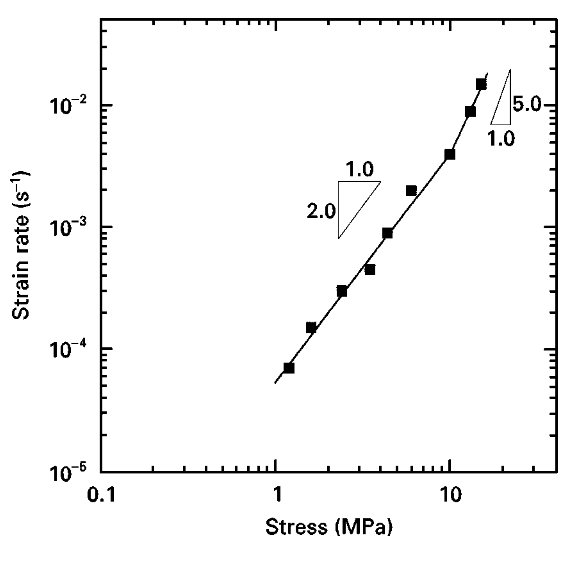

Figure 2 The influence of strain rate on the elongation to failure of the 7475 Al alloy, at 516 °C, 14 μm grain diameter.

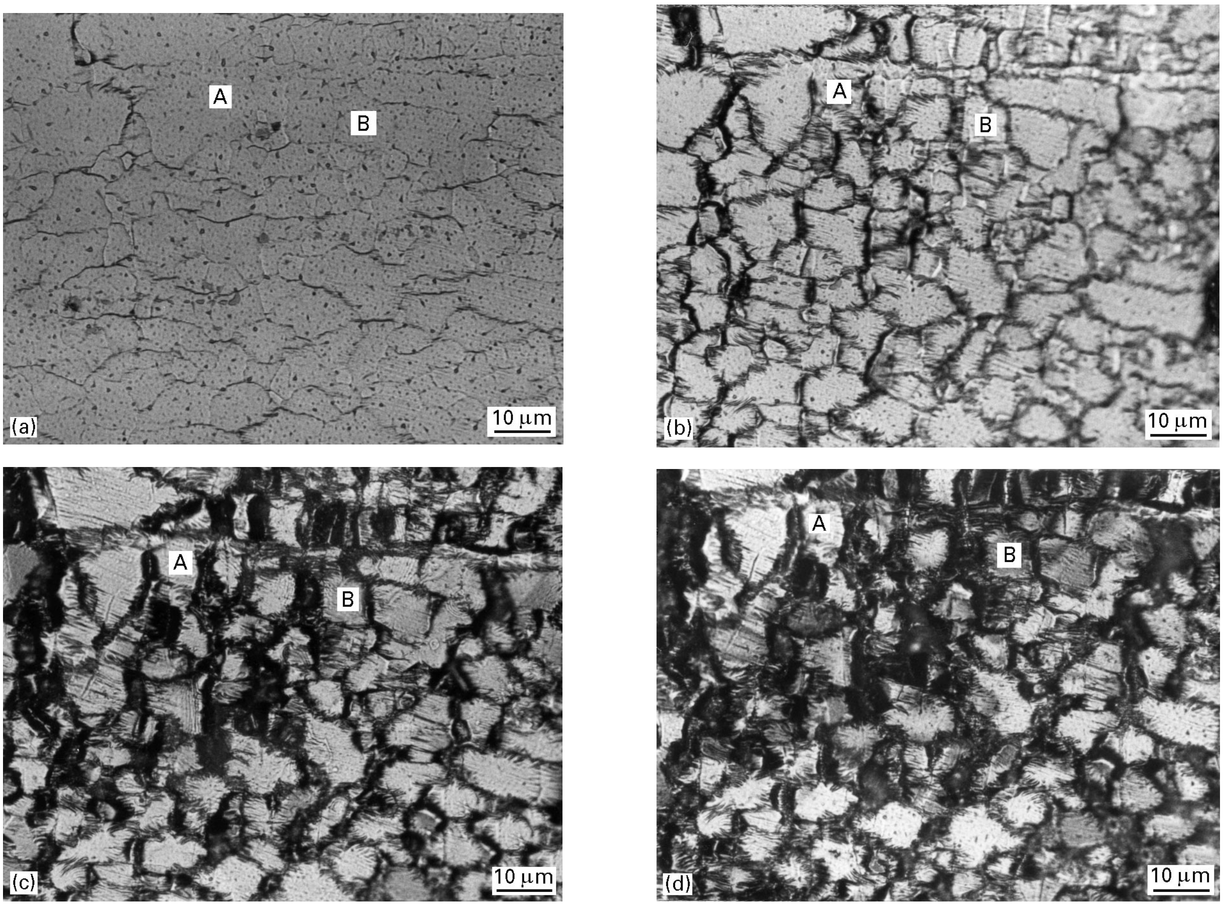

Figure 3 Optical micrographs of 7475 Al alloy after (a) 5%, (b) 20%, (c) 45%, and (d) 60% elongation at a strain rate of $2.1 \times 10^{-2}\,s^{-1}$.

recrystallization. Dynamic recrystallization has been observed within the superplastic temperature and strain-rate regime, this effect being more visible when the grain size becomes larger [12].

Based on metallographic observations, Ghosh and Raj [13] have concluded that deformation in Region III (at a strain rate of $10^{-2}\,s^{-1}$) produces the grain refinement in the 7475 Al alloy. They interpreted these observations in terms of a dynamic recrystallization mechanism. However, Wert and Varloteaux [14] pointed out that Ghosh and Raj [13] could not account for the subgrain boundary formation because grain boundaries and subgrain boundaries were not distinguishable by optical metallography. Wert and Varloteaux [14] measured the grain size by optical metallography of anodized specimens after deformation at a strain rate of $10^{-2}\,s^{-1}$. The equivalent spherical grain diameter was not changed after deformation, although extensive subgrain boundary networks were observed by transmission electron microscopy. From the results, Wert and Varloteaux [14] concluded that grain refinement by dynamic recrystallization does not occur during deformation of the 7475 aluminium alloy at 516 °C at a strain rate of $10^{-2}\,s^{-1}$, contrary to Ghosh and Raj's results [13].

Fig. 3 indicates the subgrain boundary formation after low superplastic elongations. However, as deformation proceeded, evidence for grain boundaries resulting from continuous recrystallization has been observed. The refining of the initial grain size can also be seen by a comparison of the optical micrographs after 100% elongation in the grip region (Fig. 5a) and in the gauge region (Fig. 5b). Thus, the present results agree with the suggestion by Ghosh and Raj [13].

It was suggested in superplastic 7475 Al alloy that power-law creep in the coarse grain material causes an accumulation of sufficient defect density, which allows the nucleation of new stress-free grains [13]. In many materials, this dynamic recrystallization causes the nucleation of new grains around the existing grain boundaries in a "necklace" form [15]. However, as far as this study is concerned, no indication of "necklace" recrystallization has been observed. Our results suggest that "continuous" recrystallization is involved in the refining of coarser grains of the statically recrystallized 7475 Al alloy. Continuous recrystallization is generally considered to be a recovery-dominated process, resulting in a progressive increase in grain-boundary misorientation and conversion of low-angle boundaries into higher-angle boundaries [15]. The high strain-rate deformation in the statically recrystallized 7475 Al alloy seems to result in rapid microstructural changes, which include the conversion of many low-angle grain boundaries to high-angle boundaries within coarse grains.

3.2. Two-stage strain-rate tests

Previous research on the 8091 Al–Li alloy by Gandhi *et al.* [5] shows that the superplastic elongations are higher in two-stage strain-rate tests than in a single strain-rate tests. In the two-stage strain rate tests, the

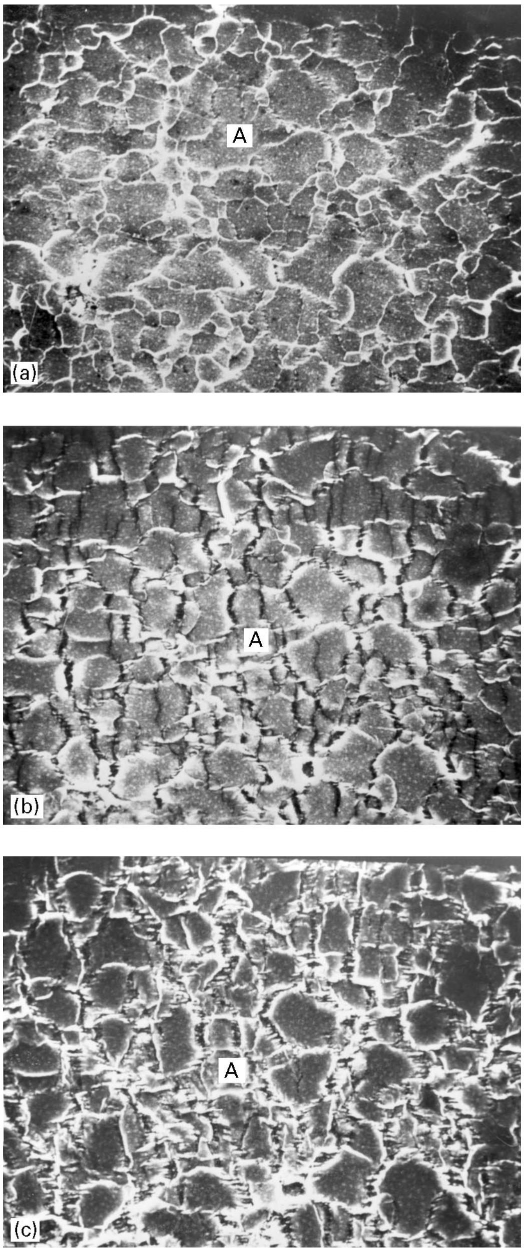

Figure 4 Scanning electron micrographs of 7475 Al alloy after (a) 5%, (b) 45%, and (c) 100% elongation at a strain rate of $2.1 \times 10^{-2}\,s^{-1}$.

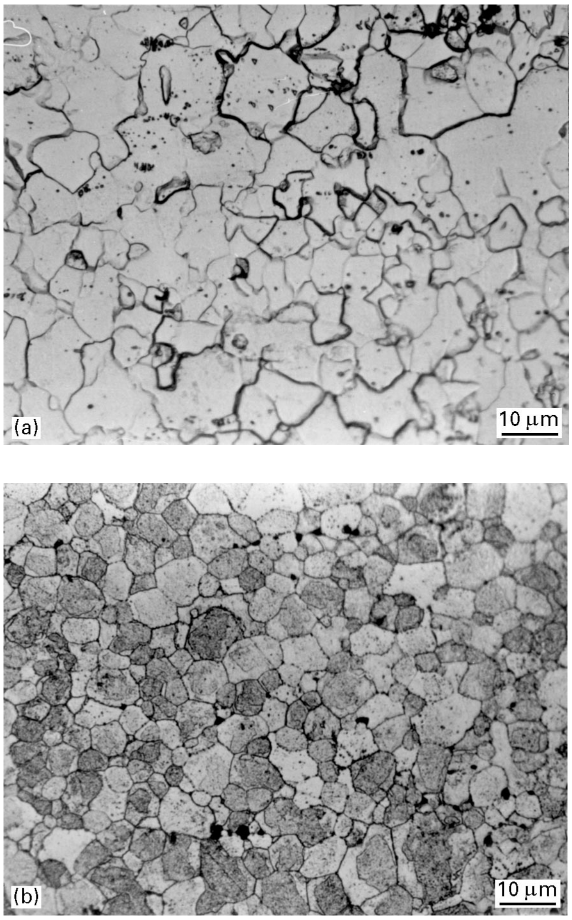

Figure 5 Optical micrographs of 7475 Al alloy after 100% elongation at 516 °C at (a) the grip region, and (b) the gauge region.

tensile sample was deformed at a higher strain rate to a predetermined strain and the strain was dropped by an order of magnitude and the test was continued until the sample failed. It was shown that the dynamic recrystallization of an initial wrought structure was occurring during superplastic deformation of the 8091 Al–Li alloy.

In the case of the aluminium alloy, the superplasticity is obtained through static (or discontinuous) recrystallization. Static recrystallization produces a stable fine grain structure prior to superplastic deformation. Two-stage strain-rate tests are performed on the 7475 Al alloy to correlate the effect of grain refinement at a higher strain rate (Fig. 3) with the effect of the second strain rate on the total elongation. To do that, determination of the optimum first strain rate and strain is required.

A few tensile tests are performed at 516 °C to optimize the first strain rate for obtaining a maximum enhancement in superplasticity. The first strain rate varies from $1.3 \times 10^{-3}\,s^{-1}$ to $1.3 \times 10^{-2}\,s^{-1}$, while the second strain rate is kept constant at $1.3 \times 10^{-3}\,s^{-1}$. The optimum first strain rate is $6.3 \times 10^{-3}\,s^{-1}$. The results are shown in Fig. 6. Two-stage strain-rate tensile tests are also performed to find the optimum strain in the first stage on the total elongation. The strain rates are kept constant at $6.3 \times 10^{-3}\,s^{-1}$ and $1.3 \times 10^{-3}\,s^{-1}$, and the first strain is varied from 0–0.69. The total superplastic elongation rapidly increases with an increase in the first strain from 0.34 to 0.47 and finally decreases above 0.5. The optimum first-stage strain is approximately 0.47.

Using the optimized first strain rate and strain, superplastic tests are performed to find effects of the second strain rate on the total elongation. Fig. 7 shows the superplastic elongations of 7475 Al as a funcion of second strain rate. Significant improvement of superplasticity by the two-stage strain rate tests is quite evident. The two-stage strain rate tests show the elongation-to-failure to be between the results for 14 μm grain size and those for 8 μm grain size. The difference in elongation observed by the two-stage strain-rate tests as compared to the tests for 14 μm grain size, might be related to a refinement of the initial grain size as shown in Figs 3 and 4.

Summarizing the above, the superplasticity of 7475 Al alloy is improved significantly by the two-stage strain-rate tests, and it might be related to the

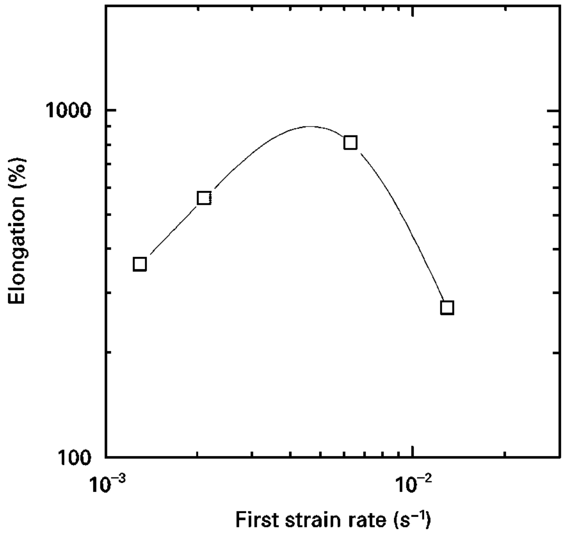

Figure 6 The influence of first stage strain rate on elongation to failure. 7475 Al at 516 °C, 14 μm grain size. $e_1 = 60\%$, $\dot{\varepsilon}_2 = 1.3 \times 10^{-3}\,s^{-1}$.

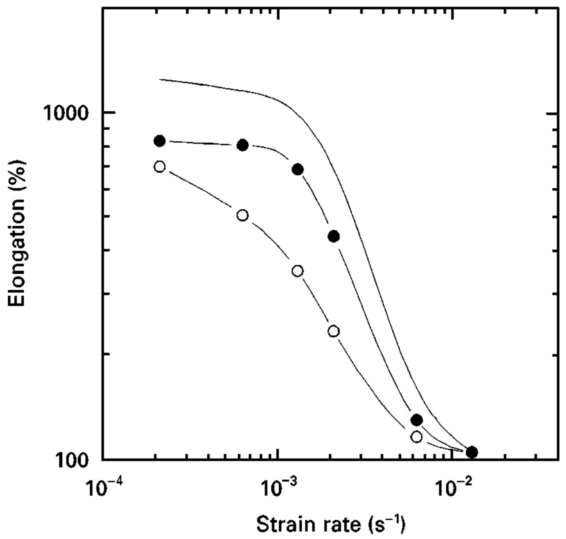

Figure 7 The influence of strain rate on the elongation to failure of 7475 Al alloy at 516 °C, (○) 14 μm diameter, $e_1 = 0\%$, (●) 14 μm diameter, $e_1 = 60\%$, $\dot{\varepsilon}_1 = 6.3 \times 10^{-3}\,s^{-1}$; (—) 8 μm diameter [2].

refinement of the initial grains at higher strain rate of $10^{-2}\,s^{-1}$.

3.3. Deformation at low strain rate

Fig. 8 shows optical micrographs of 7475 Al alloy for the same region after 20% and 40% elongation at 516 °C at an initial strain rate of $2.1 \times 10^{-1}\,s^{-1}$. The original equiaxed grains remained equiaxed, with new deformation bands formed at grain boundaries primarily normal to the tensile direction. These bands are believed to represent the grains emerging from the interior on to the surface of the specimen. It is also important to note that, as indicated by lines in Fig. 8, the increased elongation resulted from the widening of the newly formed deformation band.

Fig. 9 is a polished and etched structure of the same region of Fig. 8b. Dispersoid-free zones (DFZs) adjacent to grain boundaries primarily normal to the tensile direction, are evident. Recently, several investigations [2, 16, 17] reported the existence of DFZs in the vicinity of grain boundaries perpendicular to the tensile axis in the superplastically deformed 7XXX Al alloys. At present, the origin of DFZs, where formation shows a close similarity to structural change during diffusional flow, is not well understood. It is believed that the formation of DFZs is a genuine and unique microstructural evolution occurring during the superplastic deformation of high-strength aluminium alloy.

When a higher strain rate is applied to the specimens with DFZs, it is expected that the deformation

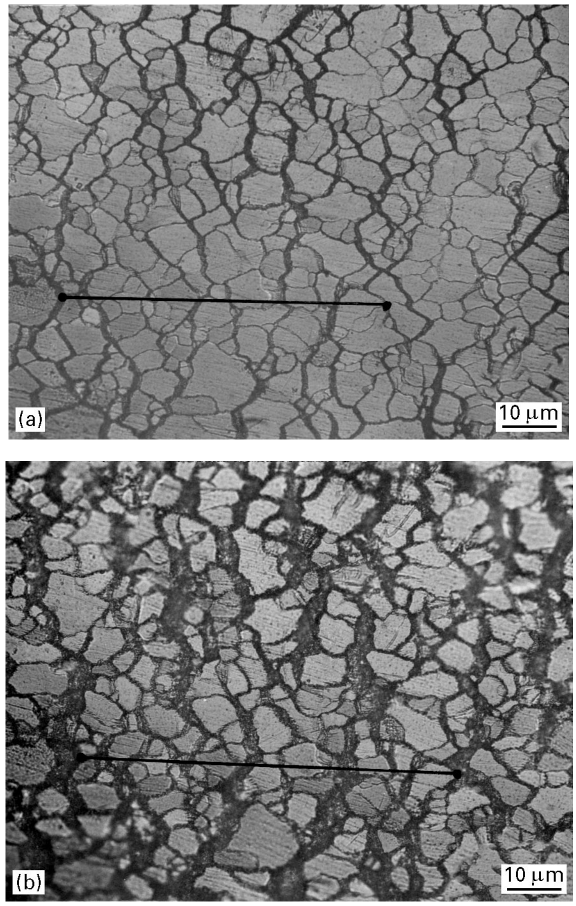

Figure 8 Optical micrographs of 7475 Al alloy for the same region after (a) 20%, and (b) 40% elongation at 516 °C at an initial strain rate of $6.3 \times 10^{-4}\,s^{-1}$.

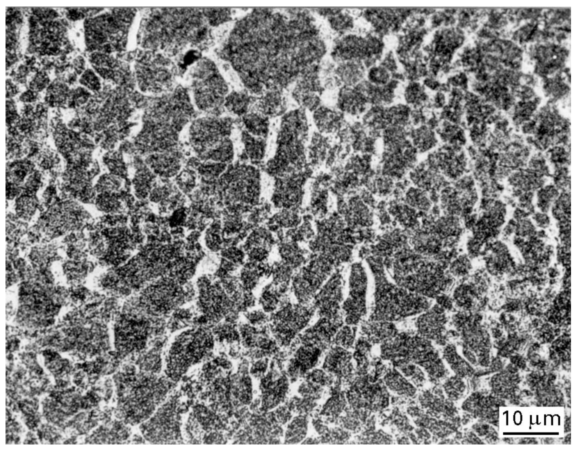

Figure 9 Polished and etched structure of the same specimen of Fig. 8b.

behaviour will be different from the specimens without DFZs. Fig. 10a shows the DFZs formed near grain boundaries after 5% elongation at lower strain rate of $2.1 \times 10^{-4}\,s^{-1}$. A higher strain rate of $2.1 \times 10^{-2}\,s^{-1}$ was applied to this specimen Fig. 10b and c show optical micrographs of the same region in a specimen at a higher strain rate of $2.1 \times 10^{-2}\,s^{-1}$ to elongations of 20% and 45%, respectively. In contrast to the results of Fig. 3, the grain refining was not observed in coarse grains at a higher strain rate. The absence of grain refining seems to be due to the concentration of plastic deformation in the weak DFZs.

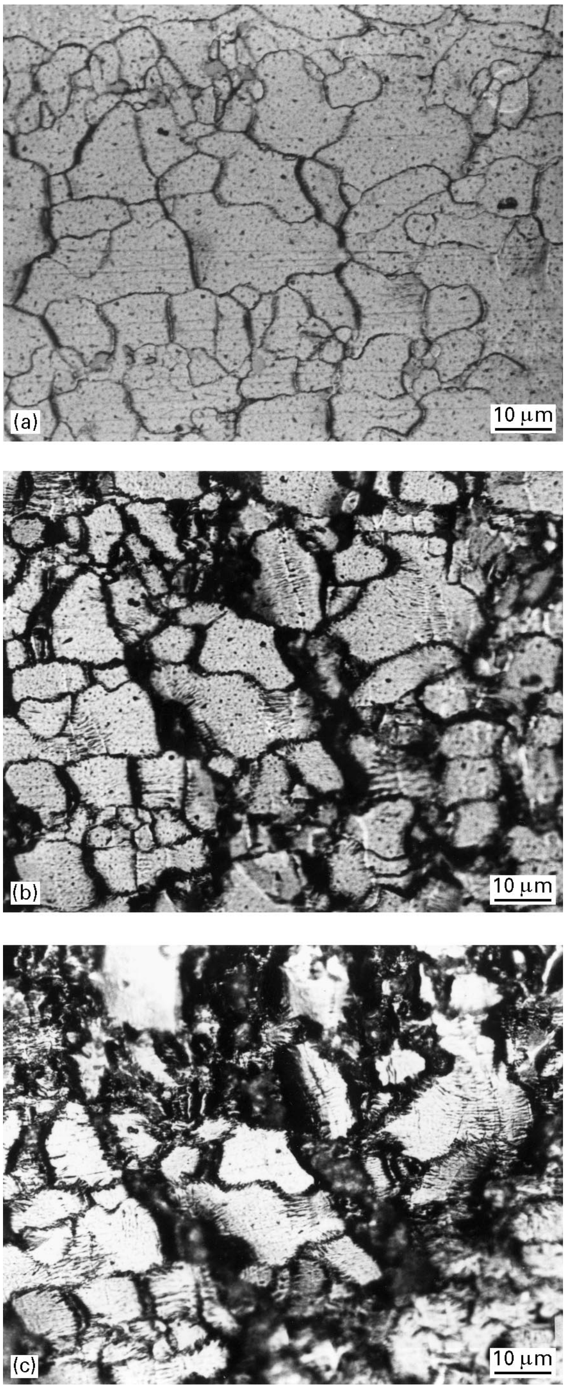

Figure 10 Optical micrographs of 7475 Al alloy showing the DFZs formed near grain boundaries. (a) Stage 1, 5% elongation at a strain rate of $2.1 \times 10^{-4}\,s^{-1}$; (b) stage 2, 20% elongation at a strain rate of $2.1 \times 10^{-2}\,s^{-1}$; and (c) stage 3, 45% elongation at a strain rate of $2.1 \times 10^{-2}\,s^{-1}$.

4. Conclusions

1. The grain refinement of the superplastic 7475 Al alloy can be obtained from superplastic tests at higher strain rate of $10^{-2}\,s^{-1}$.
2. Metallographic observations show that the average grain size is changed from 14 μm to 10 μm after 100% elongation.
3. Two-stage strain-rate tests were performed on the 7475 Al alloy to correlate grain refinement with an improvement in superplasticity. The superplasticity of 7475 Al alloy was improved significantly by the two-stage strain-rate tests, and it might be related to the refinement of the initial grains at higher strain rate of $10^{-2}\,s^{-1}$.
4. The specimens tested at a lower strain rate of $10^{-4}\,s^{-1}$ revealed the presence of DFZs near grain boundaries normal to the stress axis.

Acknowledgement

This work was supported by the Korea Science and Engineering Foundation under Grant 93-0300-04-01-3.

References

1. J. A. WERT, N. E. PATON, C. H. HAMILTON and M. W. MAHONEY, *Metall. Trans.* **12A** (1981) 1267.
2. D. H. SHIN, K. S. KIM, D. W. KUM and S. W. NAM, *ibid.* **21A** (1990) 2729.
3. B. M. WATTS, M. J. STOWELL, B. L. BAIKIE and D. G. E. OWEN, *Metal Sci.* **10** (1976) 189.
4. R. GRIMES and W. S. MILLER, in "Aluminum-Lithium Alloys II", edited by T. H. Sanders and E. A. Starke (AIME, New York, 1983) p. 153.
5. C. GANDHI, C. C. BAMPTON, A. K. GHOSH and C. E. ANTON, in "Proceedings of the 5th International Conference on Aluminum-Lithium Alloys", edited by T. H. Sanders and E. A. Starke (MCE Publications, Birmingham, UK, 1989) p. 141.
6. C. C. BAMPTON and J. W. EDINGTON, *Metall. Trans.* **13A** (1982) 1721.
7. J. PILLING and N. RIDLEY, in "Superplasticity in Crystalline Solids" (The Institute of Metals, 1989) p. 53.
8. O. D. SHERBY and J. WADSWORTH, in "ASM Materials Science Seminar on Deformation Processing and Structure", St Louis, MI, October 1982, p. 355.
9. D. H. SHIN, K.-T. PARK and E. J. LAVERNIA, *Mater. Sci. Engng* **A201** (1995) 118.
10. H. W. HAYDEN, S. FLOREEN and P. D. GOODELL, *Metall. Trans.* **3A** (1972) 833.
11. L. K. L. FALK, P. R. HOWELL, G. L. DUNLOP and T. G. LANGDON, *Acta Metall.* **13** (1986) 211.
12. A. K. GHOSH and R. RAJ, *ibid.* **34** (1986) 447.
13. *Idem*, in "Superplasticity", edited by B. Baudelet and M. Suery (CNRS, Paris, 1985) p. 11.1.
14. J. A. WERT and A. VARLOTEAUX, in "Aluminum Alloys – Their Physical and Mechanical Properties", edited by E. A. Starke and T. H. Sanders (EMAS, West Midlands, 1986) p. 1255.
15. T. SAKAI and J. J. JONAS, *Acta Metall.* **32** (1984) 189.
16. U. KOCH, in "Superplasticity in Aerospace", edited by H. C. Heikkenen and T. R. McNelly (TMS, Warrendale, PA, 1988) p. 115.
17. J. J. BRANDIN, B. HONG, A. VARLOTEAUX, M. SUERY and G. L'ESPERANCE, *Acta Mater.* **44** (1996) 2317.

Received 19 May 1997
and accepted 3 March 1998